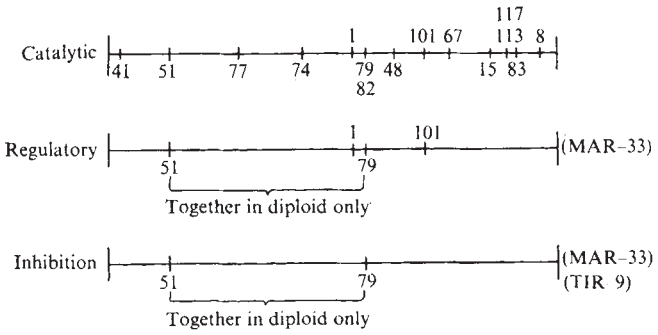

Fig. 4 Multifunctional map of the *ilv 1* gene. Each representation of the *ilv 1* gene corresponds to one of the *ilv 1* functions which are represented at the left of the corresponding cistron. Only the alleles which result in altered function are represented. The alleles above the line are of the nonsense type.

mutation near the middle of the *ilv 1* gene and that it is not suppressible (my unpublished data).

In conclusion, the results presented here strongly indicate that the *ilv 1* gene is multifunctional, coding for a product which functions in the catalysis of L-threonine to α-keto-butyrate, as well as being a positive effector in the derepression of the isoleucine-valine enzymes. I have found correlation between the isoleucine inhibition property of threonine deaminase and *ilv 1* regulatory function. Furthermore, there is intracistronic discrimination of the *ilv 1* catalytic and regulatory functions. Apparently the regulatory function of the multifunctional *ilv 1* gene represents an example of a eukaryotic regulatory gene which has been identified and partially characterised both genetically and biochemically.

I thank Dr Fritz Zimmermann for *ilv 1* auxotrophs and helpful discussions, and Dr P. T. Magee for several strains and for useful discussions. I thank Melvin Dews for technical assistance. This work was supported by a grant from the National Institutes of Health.

Received March 20, 1974.

1 Vogel, H. J. (ed.) *Metabolic regulation*, **5**, (Academic Press, New York, 1971).
2 Wolstenholme, G. E. W., and Knight, J. (ed.) *Control processes in multicellular organisms* (Churchill, London, 1970).
3 Giles, N. H., Case, M. E., Partridge, C. W. H., and Ahmad, S. I., *Proc. natn. Acad. Sci. U.S.A.*, **58**, 1453–1460 (1967).
4 Arroyo-Begovich, A., and DeMoss, J. A., *J. biol. Chem.*, **248**, 1262–1267 (1973).
5 Weiss, R. L., and Davis, R. H., *J. biol. Chem.*, **248**, 5403–5408 (1973).
6 Shaffer, B., Rytka, J., and Fink, G. R., *Proc. natn. Acad. Sci. U.S.A.*, **63**, 1198–1205 (1969).
7 Wiame, J. M., in *Current topics in cellular regulation* (edit. by Horecker, B. L., and Stadtman, E. R.) **4**, 1–20 (Academic Press, New York, 1972).
8 Kellems, R. E., and Butow, R. A., *J biol. Chem.*, **247**, 8043–8050 (1971).
9 Hartwell, L. H., Culotti, J., Pringle, J. R., and Reid, B. J., *Science*, **183**, 46–51 (1974).
10 Betz, J. L., Hereford, L. M., and Magee, P. T., *Biochemistry*, **10**, 1818–1824 (1971).
11 Bollon, A. P., and Magee, P. T., *Proc. natn. Acad. Sci. U.S.A.*, **68**, 2169–2173 (1971).
12 Bollon, A. P., and Magee, P. T., *J. Bact.*, **113**, 1333–1344 (1973).
13 Pledger, W. J., and Umbarger, H. E., *J. Bact.*, **114**, 195–207 (1973).
14 Levinthal, M., Williams, L. S., Levinthal, M., and Umbarger, H. E., *Nature new Biol.*, **246**, 65–68 (1973).
15 Calhoun, D. H., and Hatfield, G. W., *Proc. natn. Acad. Sci. U.S.A.*, **70**, 2757–2761 (1973).
16 Hatfield, G. W., and Burns, R. O., *Proc. natn. Acad. Sci. U.S.A.*, **66**, 1027–1035 (1970).
17 Goldberger, R. F., and Kovach, J. S., in *Current topics in cellular regulation* (edit. by Horecker, B. L., and Stadtman, E. R.), **5**, 295–308 (Academic Press, New York, 1972).
18 Blasi, F., Bruni, C. B., Avitable, A., Deeley, R. G., Goldberger, R. F., and Meyers, M. M., *Proc. natn. Acad. Sci. U.S.A.*, **70**, 2692–2696 (1973).
19 Katsunuma, T., Elsasser, R., and Holzer, H., *Eur. J. Biochem.*, **24**, 83–87 (1971).
20 Thuriaux, P., Minet, M., ten Beige, A. M. A., and Zimmerman, F. K., *Molec gen. Genet.*, **112**, 60–72 (1971).
21 Manney, T. R., and Mortimer, R. K., *Science*, **143**, 581–583 (1964).
22 Parker, J. H , and Sherman, F , *Genetics*, **62**, 9–22 (1969).
23 Zimmerman, F. K., Schmidt, I., and ten Beige, A. M. A., *Molec. gen. Genet.*, **104**, 321-330 (1969).
24 Magee, P. T., and Herefore, L. M., *J. Bact* , **98**, 857–862 (1969).

letters to nature

Cosmogony of the asteroidal belt

WE have to derive the state of partial corotation in a way which, by being very simple, stresses its character as a basic state in cosmic plasma dynamics. We also substitute the mass density (m, a) for the number density (n, a) in the plot of asteroids, as a function of their semimajor axis a. This gives a better definition to the limits of the main belt, and demonstrates more clearly that the asteroids—like the Saturnian rings—have condensed from a partially corotating plasma.

If a rotating body has an axisymmetric dipole field and is surrounded by a plasma, and if the electrical conductivity of the body and of the plasma is infinite, the plasma will rotate with the same angular velocity Ω as the body; the magnetic field lines are 'frozen-in'. This idealised model is, however, not applicable to cosmic problems because celestial bodies have gravitation, and the plasma is subject both to that and to the centrifugal force produced by the rotation[1–4]. Moreover, the 'frozen-in' picture is seldom applicable in astrophysics[4–7]. The assumption of infinite conductivity is unrealistic, because electric fields parallel to the magnetic field play an important role[8,9]. It is now evident that the magnetosphere is to a high degree uncoupled from the ionosphere[10].

This means that instead of a plasma corotating with an angular velocity $\omega = \Omega$, we have typically a 'partial corotation' with $\omega < \Omega$ (refs 3 and 4). The rotational velocity is given by the condition that the centrifugal force, $\mathbf{f}_c$, the gravitation, $\mathbf{f}_g$, and the electromagnetic force, $\mathbf{f}_B$, acting on a plasma element should balance each other, so that

$$\mathbf{f}_c + \mathbf{f}_g + \mathbf{f}_B = 0 \qquad (1)$$

(We assume that the plasma temperature is so low that pressure and diamagnetic effects can be neglected—see Fig. 1.) If M_c is the mass of the central body, κ the constant of gravitation, B the magnetic field deriving from a dipole with moment a, m the mass of a plasma element, I the current through it, and $\mathbf{x}_0$ a unit vector perpendicular to the axis, there is in a coordinate system (r, λ) in the meridian plane of the dipole:

$$\mathbf{f}_c = \omega^2 m r \cos\lambda \, \mathbf{x}_0 \qquad (2)$$

$$\mathbf{f}_g = (\eta M_c m / r^3)(-\mathbf{r}) \qquad (3)$$

$$\mathbf{f}_B = \mathbf{I} \times \mathbf{B} \qquad (4)$$

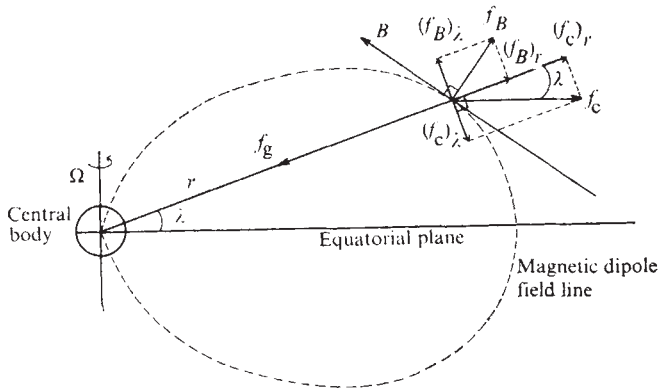

Fig. 1 Configuration of partial corotation. Equilibrium between gravitation $\mathbf{f}_g$, centrifugal force $\mathbf{f}_c$, and electromagnetic force $\mathbf{f}_B = \mathbf{I} \times \mathbf{B}$, means that $\mathbf{f}_g + \mathbf{f}_c + \mathbf{f}_B = 0$. Because $(f_c)_\lambda + (f_B)_\lambda = 0$, the geometry of the dipole field requires that $(f_c)_r = 2(f_B)_r = 2/3(-f_g)$. *a*, Central body; *b*, magnetic dipole filed line.

In a dipole field $B_r = -(2a/r^3)\sin\lambda$, $B_\lambda = (a/r^3)\cos\lambda$, and so from equations (1)–(4) (for $\lambda \neq 0$)

$$f_c = 2aI/r^3$$

and

$$f_g = [f_c + (Ia/r^3)]\cos\lambda$$

showing that: $(f_c)_r = 2(f_B)_r = (2/3)\,|f_g|$. Thus the gravitational force is compensated to 2/3 by the centrifugal force, and to 1/3 by the electromagnetic force. The factor 2/3 is given by the geometry of a dipole field.

If condensation of grains (planetesimals) takes place from a partially corotating plasma, and the resulting grains are so large that the electromagnetic forces become small compared to f_c and f_g, then they will move in Kepler orbits. As the centrifugal force does not fully compensate the gravitation, the condensed grains will move in ellipses with eccentricity, $e = 1/3$ (refs 1–4). If a large number of grains have condensed in the neighbourhood of the central body and they collide with one another, the eccentricities of their orbits will diminish, so that eventually they will all move in more circular orbits, with a semimajor axis with a length which is 2/3 the distance to the point where the condensation occurred.

There are reasons to believe that condensation from a partially corotating plasma was a basic process in the formation of the Solar System. In fact, the structure of the Saturnian ring, and of the asteroid belt can be understood in this way[1–3,11]. The factor 2/3 occurs in two places in the Saturnian ring system, and in two places in the asteroid belt. In the latter case the usual (*n*, *a*) diagram of asteroids has been used, giving the number density, *n*, of asteroids as a function of their semimajor axes, *a*.

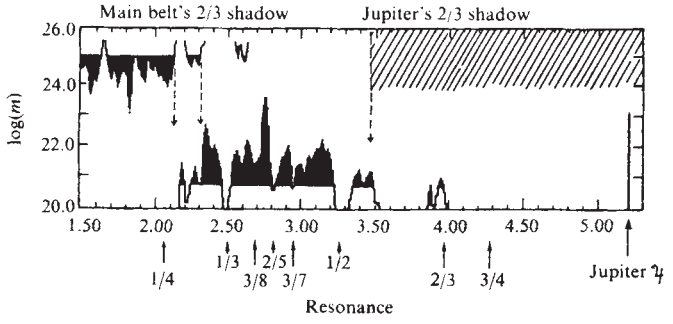

Fig. 2 The smoothed (*m*, *a*) diagram. The curve has been smoothed with the weight function 1:3:5:3:1. Mass distribution in unit of gram within a radial distance interval of $\Delta a = 0.01$ AU. In order to emphasise the log scale, high density regions are darkened. The same diagram diminished by a factor 2/3 and turned upside down is shown above, in order to demonstrate the 'shadow' effect which produces the inner cutoff of the asteroidal belt. Similarly Jupiter's 'shadow', which generates the outer cutoff, is shown. Kirkwood gaps from Jupiter resonances are arrowed.

The diagram (*n*, *a*) only gives an approximate picture of the mass distribution in the asteroid belt. We have now, however, calculated an (*m*, *a*) diagram, giving the mass distribution. We have assumed that all asteroids have the same albedo and density, so that we can put their mass proportional to (brightness)$^{3/2}$ (Fig. 2).

The (*m*, *a*) diagram shows the Kirkwood gaps, especially at 1/2 and 1/3, somewhat more clearly than the usual (*n*, *a*) diagram.

The limits of the main belt at $a = 2.15$ and 3.49 are also sharper (especially because a large number of asteroids below $a = 2.15$ have a negligible mass).

In order to study the effect of the fall-down ratio, 2/3, the (*m*, *a*) diagram, diminished by a factor 2/3, is shown reversed in the upper part of Fig. 2.

The diagram shows that the whole main belt is located below 2/3 of Jupiter's orbit, which means that the main belt asteroids may have derived from condensation which took place inside Jupiter's orbit down to $a = 3.49$. At this limit plasma would have condensed directly on already existing asteroids (or asteroidal grains), which therefore produced a 'shadow' at 2/3 this distance. As the diagram shows, there is a marked drop in mass density at $2/3 \times 3.49 = 2.32$. Above the 1:2 Kirkwood gap however, the mass density does not seem to be large enough to make the plasma density drop to zero. That does not occur until the 'shadow' of the bulk of asteroids below 3.20 appears at 2.13 (that is, $2/3 \times 3.20$).

There is no other known way to explain the upper and lower limits of the main belt.

The only asteroids outside the main belt which are massive enough to appear in the diagram are the Hildas, at $a = 3.95$ AU. As 5.9 AU ($3/2 \times 3.95$) exceeds Jupiter's distance from the Sun (= 5.2) they must have condensed outside Jupiter's orbit. When falling down in ellipses with $e = 1/3$ they avoided capture (or dispersal) by Jupiter because they were commensurable with Jupiter's orbit period to a degree of 2/3 that kept them from coming close to Jupiter. (Compare the Neptune–Pluto resonance and similar cases[12].

The 2/3 ratio is found in three places in the asteroid (*m*, *a*) plot (Fig. 2). In fact, the observed ratios agree with the theoretical value to within 1%. Including the two occurrences in the Saturnian ring system there are five cases which confirm that the condensation from a plasma in partial corotation was an important process in the formation of the Solar System.

The mass distribution of the asteroids is not altogether explained by the resonances and the 2/3 fall-down. For example, there is a very strong peak at 2.75 which includes Ceres and Pallas, and a secondary peak at 2.36 which includes Vesta. These may result from a later evolution which concentrates mass through a process which eventually leads to the formation of planets.

This research is funded by the Planetology Program Office, NASA.

HANNES ALFVÉN
WING-HUÉN IP

Department of Applied Physics and Information Science, University of California, San Diego, La Jolla, California 92037

MARTIN D. BURKENROAD

Department of Earth Sciences, Tulane University, New Orleans, Louisiana 70118

Received February 4, 1974.

[1] Alfvén, H., *Stockh. Obs. Annl.*, **14**, No. 2 (1942); **14**, No. 5 (1943); **14**, No. 9 (1944).
[2] Alfvén, H., *On the Origin of the Solar System* (Oxford University Press, Oxford, 1954).
[3] Alfvén, H., *Icarus*, **7**, 387 (1967).
[4] Alfvén, H., and Arrhenius, G., *Astrophys. Space Sci.*, **21**, 117 (1973).
[5] Alfvén, H., and Fälthammar, C. G., *Cosmical Electrodynamics Fundamental Principles* (Oxford University Press, Oxford, 1963).

[6] Alfvén, H., *Annls Géophys.*, **24**, 1 (1968).
[7] Alfvén, H., in *Relations between Cosmic and Laboratory Plasma Physics: Cosmic Plasma Physics* (edit. by Schindler, K.), 1 (Plenum, New York, 1972).
[8] Fälthammar, C.-G., *Space Sci. Revs.*, **15**, 803 (1974).
[9] Block, L. P., *Cosmic Electrodynamics*, **3**, 349 (1972).
[10] Bostrom, R., in *Magnetospheric Physics* (edit. by McCormac, B. M.), (Reidel, Dordrecht, in the press).
[11] Alfvén, H., *Icarus*, **8**, 75 (1967).
[12] Alfvén, H., and Arrhenius, G., *Astrophys. Space Sci.*, **8**, 338 (1970).

A Lagrangian community?

IT seems that it may be economically feasible, within the limits of the technology of this decade, to establish at one of the Lagrange libration points of the Earth-Moon system (called here L_5) a habitat capable of supporting and maintaining some 10,000 people. Projections indicate that this habitat, using free solar energy and the rich mineral resources of the lunar surface, could construct a still larger habitat, in a progression leading, possibly within 30 yr from now, to communities of from 10^5 to 10^7 people. These communities could be as comfortable as the most desirable parts of the Earth, with natural sunshine, controlled weater, normal air, apparent gravity and complete freedom from pollution. Replication of these communities could lead to the exponential growth of new land area, with a growth rate more rapid than that of the total human population.

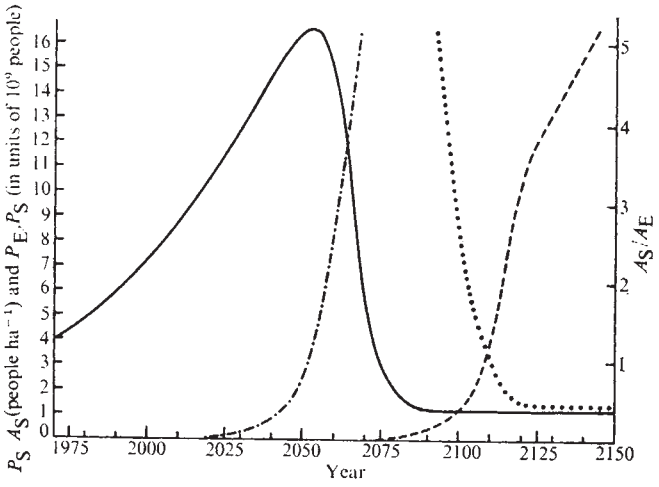

Fig. 1 A graph, technically realisable in my opinion, showing that most industry could be removed from the biosphere of the Earth within a century. The graph is based on a "worst-case" assumption: no reduction of the population growth rate either on earth or in the space communities. P_E is the population on earth, P_S the population in space, A_S/A_E the ratio of land area in space (all usable) to the total land area of Earth. Changes within wide limits in the assumed input numbers do not affect reaching a solution stable in P_E and P_S/A_S. The final stable value of P_E (1.2×10^9 people) is equivalent to the 1910 value. —, P_E; — · —, P_S; . . . . ., P_S/A_S; – – –, A_S/A_E.

A technically possible time-development is shown in Fig. 1, not as a prediction but as an illustration of the power of the technique.

Economic feasibility is defined here as the achievement of an overall cost less than or equal to that of the Apollo project. A reduction in the design size of the first habitat, with a corresponding reduction in the size of its population, would result in some further reduction in the estimates.

The solutions to several problems were necessary in order to achieve this feasibility:

(*a*) Geometry: A physical arrangement has been found which would allow the use of natural sunlight for industry, farming and the maintenance of an attractive, earthlike environment with normal day/night and seasonal cycles.
(*b*) Transport from the earth to L_5: A reconfiguration of hardware already under development for the space-shuttle (to be operational by 1980) seems adequate to transport the necessary minimum of materials from earth.
(*c*) Water: The combination, at L_5, of hydrogen from the earth with oxygen from the abundant oxides of the lunar surface effects an important saving of a factor 9 in the mass of material needed from earth per unit mass of water at L_5.
(*d*) Materials: Obtaining nearly all the mass of the habitat from the moon appears essential for economy. Two alternative designs have been studied for the acceleration of lunar materials to the 2.4 km^{-1}s escape velocity of the moon. Both designs depend on the vacuum environment of the moon. Neither is conventional, but the technology of the present decade would suffice for either.

The ultimate benefits of this new possibility depend on the production of successively larger communities by a workforce which is housed, fed and maintained within the communities rather than on earth, and so to the eventual achievement by the communities of the ability to sustain their own growth by the construction of new lands and production facilities from lunar and asteroidal material.

These studies have been discussed in lectures at a number of universities during the past 18 months. Knowledge of the work has therefore spread, additional people have joined the effort, and recent progress has been rapid. On May 10, 1974, the first public meeting on this topic was held at Princeton University.

Detailed information on these studies will be found in forthcoming publications in *Physics Today* and in *Icarus*.

GERARD K. O'NEILL

Department of Physics,
Princeton University,
Princeton, NJ 08540

Intensity of the near infrared OH airglow

THE OH airglow was studied from the balloon-borne telescope Thisbe on three flights launched in 1971 and 1972 from the NCAR balloon flight station, Palestine, Texas (32°N, 95°W). The principal goal of these flights has been the measurement of the zodiacal light in the near infrared[1] with the airglow as a troublesome foreground contribution which had to be determined carefully.

The measurements have been performed from a float altitude of 32 km at wavelengths $\lambda = 0.82$, 2.1, and 2.4 μm with half power bandwidths $\Delta\lambda = 0.023$, 0.1 and 0.1 μm respectively. For the shorter wavelengths a straightforward photometer with a multiplier as detector has been used. The larger wavelengths were measured by a dry ice cooled PbS-photometer. The field of view of both photometers was 2° in diameter. The 0.82 μm photometer was calibrated by observations of 33 stars. The PbS-photometer was calibrated before the flight by a 240 K blackbody and during the flight by the star α-Ori

$$(I_{2.1\ \mu m} = 1.9 \times 10^{-12} \text{W cm}^{-2}\ \mu\text{m}^{-1};$$
$$I_{2.4\ \mu m} = 1.3 \times 10^{-12} \text{W cm}^{-2}\ \mu\text{m}^{-1}).$$

The airglow intensity was determined from several elevation scans. As an example Fig. 1 shows the result of an elevation scan at $\lambda = 2.1$ μm.

A van Rhijn curve for an emission altitude of 92 km was fitted to the data. The resulting zenith intensities at all measured wavelengths are listed in Table 1.